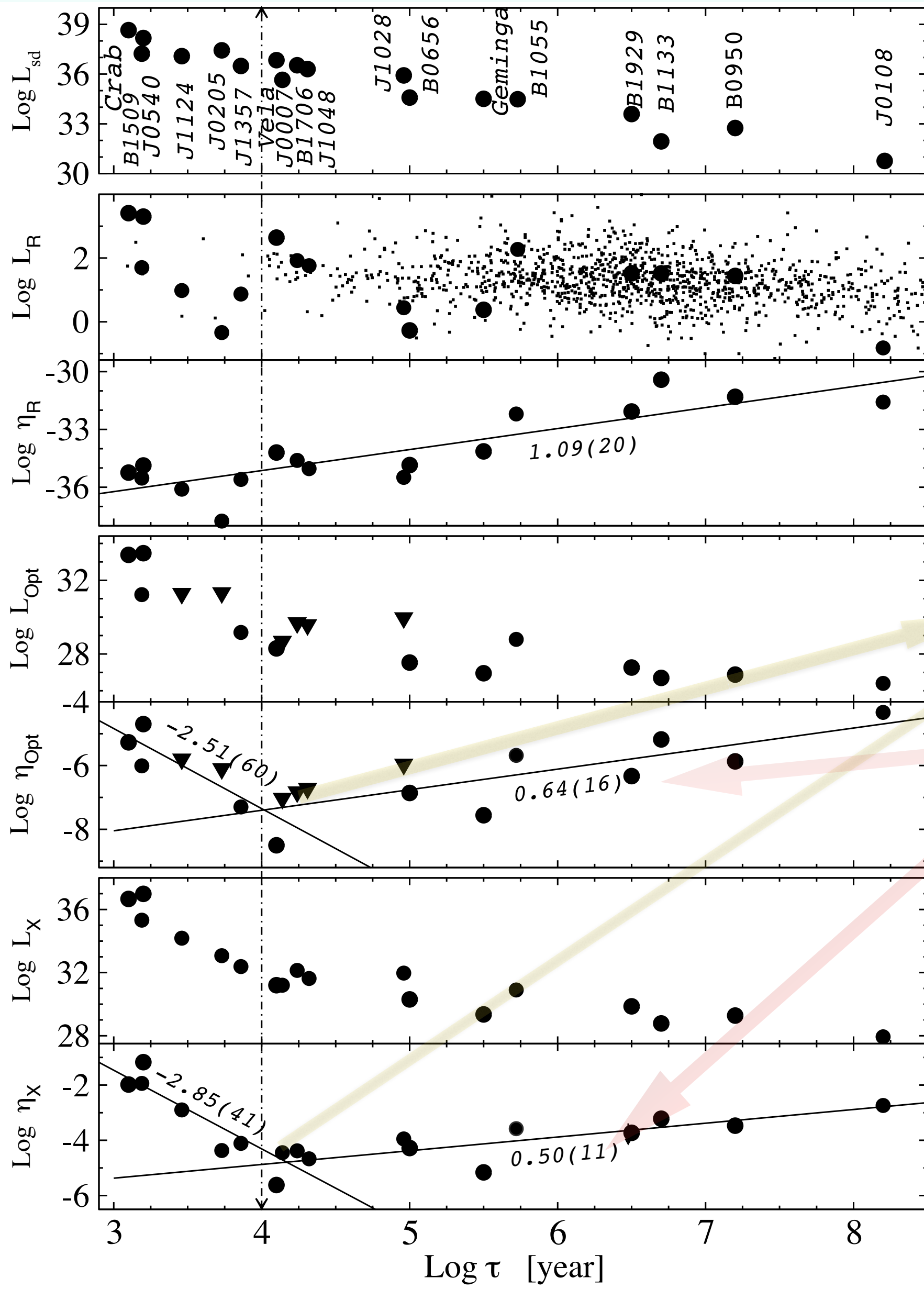


Radiation efficiencies of the pulsars (current update).

Zharikov S. V.

Observatorio Astronomico Nacional, Instituto de Astronomia,

18 pulsars
(12 in optical range + 6 upper limits)
~10³- ~10⁹ yy.



From top to bottom: evolution of the pulsar spin-down, radio, optical and X-ray luminosity, and respective efficiencies, as a function of the dynamical age. The full circles show the luminosity and radiation efficiency of pulsars with optical counterparts, while the triangles mark upper limits. The points show the radio luminosity of the rest of radio pulsars taken from the ATNF pulsar catalogue (Manchester et al. 2005). The data was taken from Zharikov et al. (2006) and updated using Danilenko et al. (2012), Mignani et al. (1999, 2009, 2010, 2011, 2013), Shibanov et al. (2008), Zharikov et al. (2008a, 2008b) and references there in. The vertical line marks the age when the change of the behaviour of the radiation efficiency occurs.

- Increasing of number of optical detected pulsars (or upper limits on its optical fluxes) confirmed that these pulsars show significantly non-monotonic behaviours of the optical and X-ray efficiencies with pulsar's age and show a pronounced minimum at the beginning of the middle-age epoch ($\tau \sim 10^4$ yr).
- At same time ($\tau \sim 10^4$ yr) also γ -ray efficiency increases about order of magnitude.
- Beginning from this age the contribution of black body radiation in X-ray data from NS surface (whole or a polar spot) is ranged of $\eta_{bb} \sim 10^{-2} - 2$, that is significantly larger than in case of younger ($\tau < 10^4$ yr) pulsars ($\eta_{bb} \sim 10^{-4} - 10^{-3}$).
- The origin of the efficiency behaviours probably caused by the switch between neutrino and photon cooling stages that affects the distribution of relativistic particles in the pulsar magnetosphere.
- The optical and X-ray efficiencies comparably for younger and older pulsars.
- New data also confirmed the strong correlation between the optical and 0.5–8 keV X-ray luminosities of these pulsars. This implies the same origin of their non-thermal emission in both spectral domains.

Table 1

The dynamical ages $\tau = P/2\dot{P}$, distances d , spindown luminosities \dot{E} (or L_{sd}), and observed non-thermal luminosities in the radio, L_R , optical, L_{opt} , X-rays, L_X , and γ -rays, L_γ , of seven radio pulsars detected in the optical range (Zharikov et al., 2002, 2004)

Source	log τ (yr)	d (pc)	log \dot{E} (erg s ⁻¹)	log L_R^a (mJy kpc ²) 408 MHz	log L_{opt} (erg s ⁻¹) B-band	log L_X (erg s ⁻¹) 2–10 keV	log L_γ (erg s ⁻¹) ≥ 400 MeV
Crab	3.1	2.0×10^3	38.65	3.41(4)	33.23(5)	36.67 ⁽⁺²⁰⁾ ₍₋₂₆₎	35.7 ⁽⁺¹⁾ ₍₋₁₎
B0540-69	3.2	5.0×10^4	38.17	3.30(9)	33.47(15)	36.99 ⁽⁺¹⁹⁾ ₍₋₂₃₎	≤ 35.97
Vela	4.1	293 ⁽⁺¹⁷⁾ ₍₋₁₇₎	36.84	2.64(20)	28.3(3)	31.2 ⁽⁺³⁶⁾ ₍₋₃₈₎	33.9 ⁽⁺³⁾ ₍₋₃₎
B0656+14	5.0	288 ⁽⁺³³⁾ ₍₋₂₇₎	34.58	-0.27(9)	27.53(8)	30.30 ⁽⁺³⁶⁾ ₍₋₃₈₎	32.37 ⁽⁺¹⁰⁾ ₍₋₁₀₎
Geminga	5.5	153 ⁽⁺²³⁾ ₍₋₂₄₎	34.51	0.375 ⁽⁺²⁷⁾ ₍₋₂₃₎	26.95 ⁽⁺¹⁶⁾ ₍₋₁₀₎	29.35 ⁽⁺³⁸⁾ ₍₋₃₆₎	32.95 ⁽⁺¹⁰⁾ ₍₋₁₀₎
B1929+10	6.5	361 ⁽⁺⁸⁾ ₍₋₈₎	33.59	1.52(5)	27.26 ⁽⁺²⁰⁾ ₍₋₃₃₎	29.86 ⁽⁺¹³⁾ ₍₋₁₃₎	≤ 32.57
B0950+08	7.2	262(5)	32.75	1.44(16)	26.88(8)	29.28 ⁽⁺¹³⁾ ₍₋₁₈₎	≤ 32.51

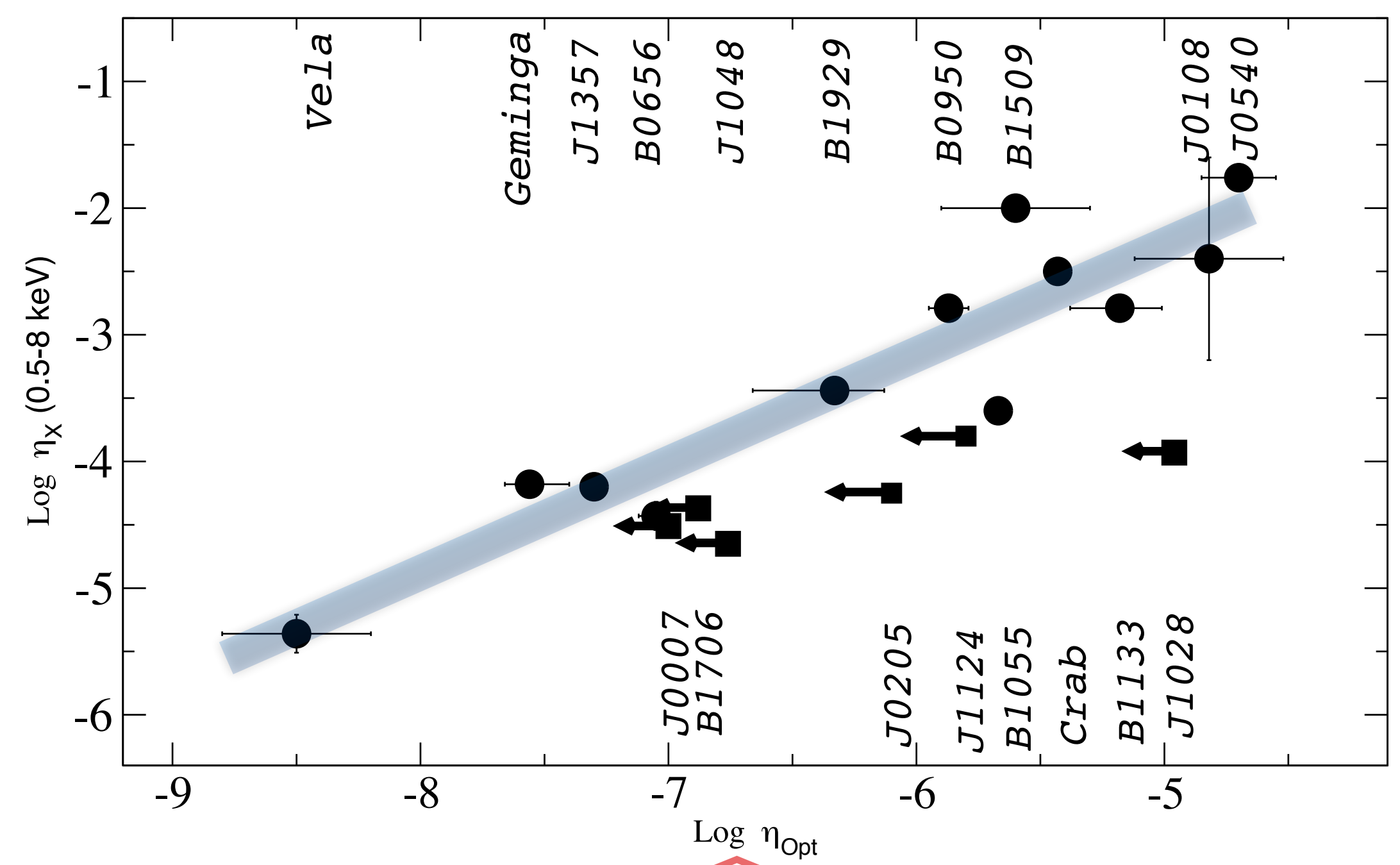
Figures in brackets are $\pm 1\sigma$ uncertainties of the values.

^a The radio luminosity is defined traditionally as $L_R = S_{408} d^2$ (mJy kpc²), where S_{408} is the observed flux density from a pulsar at 408 MHz in mJy, and d is its distance in kpc. At a typical radio band FWHM of about 100 kHz, the conversion factor to standard luminosity units is $\approx 9.51 \times 10^{21}$ (erg s⁻¹) / (mJy kpc²).

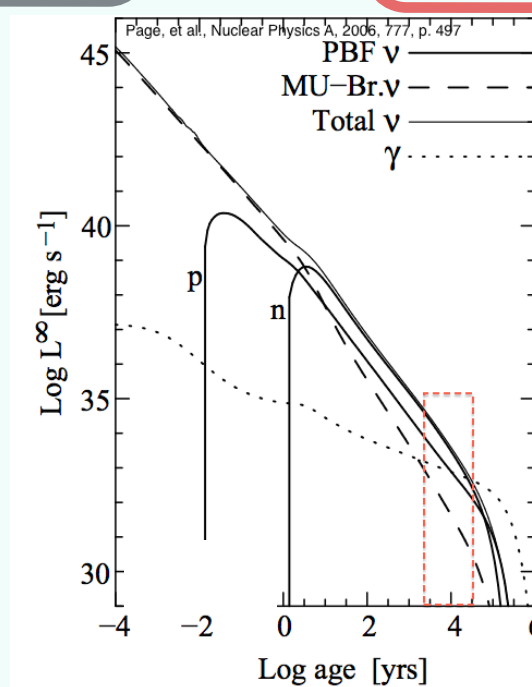
Abstract: Eighteen pulsars with optical counterparts or with significantly deep upper limits on the optical luminosity are known currently. Using available multi-wavelength data for these pulsars we reanalyze the efficiencies of the conversion of the pulsar spin-down power L_{sd} into the observed non-thermal luminosity L in different spectral domains. This sample of pulsars confirms the non-monotonic evolution of the pulsar radiation efficiency $\eta = L/L_{sd}$ in the optical and X-ray domains (Zharikov et al. 2006). There is a clear evidence of a change in the behavior of the optical and X-ray efficiencies around $\tau \sim 10^4$ years. Efficiencies η_{opt} and η_X initially decrease before starting to flatten or increase at larger ages. The timescale $\tau \sim 10^4$ years is comparable to the transition between neutrino and photon cooling stage (Yakovlev et al. 2004, and references therein) in neutron stars. The change of the cooling stage probably affects the distribution of relativistic particles in the pulsar magnetosphere, which is reflected in the dependence of the optical/X-ray efficiency on the pulsar age. The slopes of the time evolution of $\eta_{opt}(\tau)$ and $\eta_X(\tau)$ after 10^4 years are practically similar and compatible with that of $\eta_R(\tau)$.

There is a clear evidence of a change in the behaviour of the optical and X-ray efficiencies, which initially seem to decrease before starting to flatten or increase at larger ages. The turnover is located around $\tau \sim 10^4$ years.

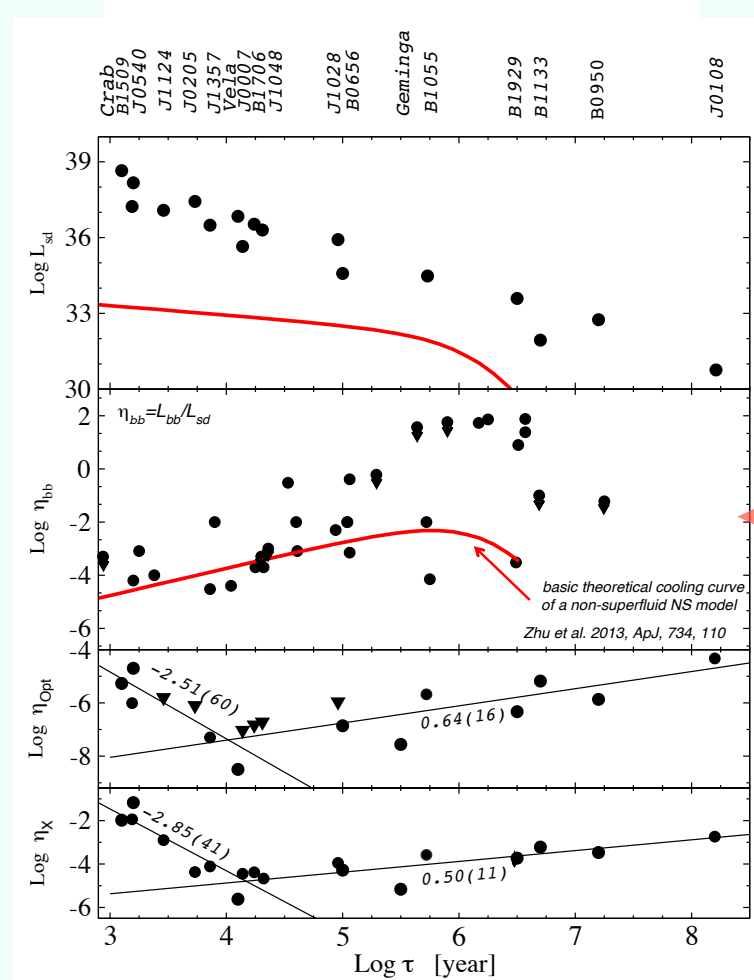
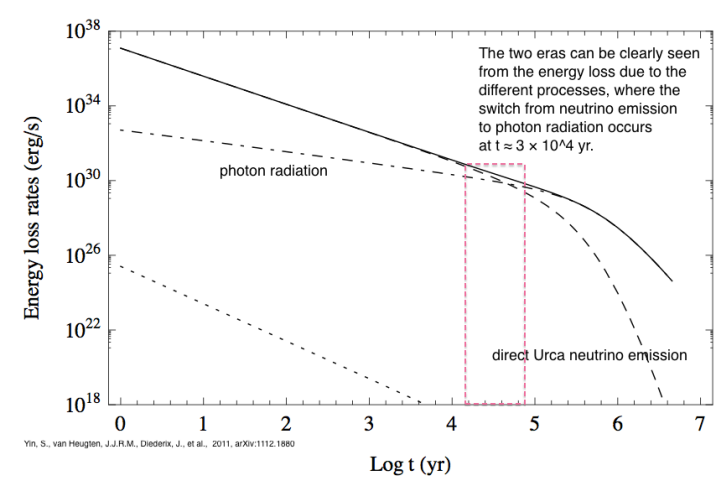
The slopes of the time evolution of $\eta_{opt}(\tau)$ and $\eta_X(\tau)$ after 10^4 years are practically similar and compatible with that of $\eta_R(\tau)$.



The correlation between the optical and 0.5–8 keV X-ray luminosities



The two eras can be clearly seen from the energy loss due to the different processes, where the switch from neutrino emission to photon radiation occurs at $\tau \sim 3 \times 10^4$ yr.



X-RAY OBSERVATIONS OF HIGH-B PULSAR 3718–3718

SURFACE TEMPERATURES MEASURED FOR SEVEN OF PULSARS, NORMAL PULSARS, AND XINIS.

PBR	τ (yr)	B (G)	R^2 (km)	R^2 (km)	R^2 (km)	R^2 (km)	reference
B0950+08	18000	2.4×10^7	<41.0	100.3	<0.06	100.3	Becker et al. (2004)
B1929+10	3100	2.2×10^7	200.2	103.3 ± 0.0(0.4)	2×10^{-4}	103.3	Mignani et al. (2009)
B0540-69	40	7.3×10^7	181 ± 3	$2.23 \pm 0.01(0.1)$	0.01	181 ± 3	Neeb et al. (2007)
B0656+14	564	8.4×10^7	200 ± 2	$0.12 \pm 0.01(0.1)$	7×10^{-4}	200 ± 2	McGowan et al. (2005)
B0656+14	4000	9.6×10^7	200 ± 2	$0.12 \pm 0.01(0.1)$	<0.10	200 ± 2	Becker et al. (2005)
B1055-52	535	1.1×10^8	68 ± 3	12.31 ± 0.08	0.01	68 ± 3	De Luca et al. (2005)
B0656+14	342	1.6×10^7	41.4 ± 0.1	9.1 ± 0.2	9×10^{-4}	41.4 ± 0.1	Z. Mészáros et al. (2001)
B1929+10	23	1.7×10^7	150	100.05	<0.001	150	Kemp et al. (2009)
B1929+10	114	1.8×10^7	70 ± 2	7.0 ± 0.1	7×10^{-4}	70 ± 2	Z. Mészáros et al. (2001)
B1929+10	21	2.8×10^7	97 ± 1	7.8 ± 0.5	2×10^{-4}	97 ± 1	Paolino et al. (2009)
B1929+10	18	3.1×10^7	143 ± 14	3.6 ± 0.0(0.2)	4×10^{-4}	143 ± 14	McGowan et al. (2005)
B0950+08	11	2.4×10^7	93 ± 3	$5.1 \pm 0.1(0.1)$	4×10^{-4}	93 ± 3	Manzoni et al. (2007)
B1929+10	20	2.5×10^7	<0.01	102.2	< 5×10^{-4}	<0.01	Crab pulsar (2006)
B0950+08	24	2.8×10^7	112 ± 9	110.2	9×10^{-4}	112 ± 9	Shen et al. (2005)
B1929+10	111	4.7×10^7	56.0 ± 0.9	21 ± 0.3	0.01	56.0 ± 0.9	De Luca et al. (2005)
B1929+10	7.2	7.8×10^7	100 ± 2	104.1	2×10^{-4}	100 ± 2	C. Cheng et al. (2001)
B1929+10	41	9.9×10^7	100 ± 25	78.3	8×10^{-4}	100 ± 25	McGowan et al. (2005)
B1929+10	0.36	3.8×10^7	<0.72	102.2	< 5×10^{-4}	<0.36	Crab pulsar (2006)
B1929+10	88	1.6×10^7	180 ± 20	180 ± 20	0.005	180 ± 20	Zhu et al. (2007)
B1929+10	3000	1.0×10^7	100 ± 4	4.0 ± 0.4	0.01	100 ± 4	Becker et al. (2005)
B1929+10	197	2.1×10^7	<73.0	100.7	<0.6	<73.0	Kemp et al. (2009)
B1929+10	3000	1.0×10^7	100 ± 4	4.0 ± 0.4	0.01	100 ± 4	Becker et al. (2005)
B1929+10	3000	2.5×10^7	87 ± 11	100.7	0.01	87 ± 11	Kemp et al. (2009)
B1929+10	700	2.7×10^7	<104	64.0 ± 4	<0.8	<104	Schepers et al. (2001)
B1929+10	442	2.7×10^7	<130	100.2	<0.8	<130	Kemp et al. (2009)
B1929+10	1300	3.4×10^7	100 ± 2	4.0 ± 0.2	0.01	100 ± 2	Schepers et al. (2001)
B1929+10	1.8	4.1×10^7	210 ± 30	$2.7 \pm 0.7(0.4)$	8×10^{-4}	210 ± 30	Stef. Mészáros & Komar (2008)
B1929+10	100	1.0×10^7	40 ± 3	3.0 ± 0.1	0.01	40 ± 3	Hobart et al. (2005)
B1929+10	0.88	4.9×10^7	<200	100.2	< 5×10^{-4}	<200	Lipunov et al. (2011)
B1929+10	117	5.0×10^7	120 ± 20	2.1 ± 0.4(0.4)	0.4	120 ± 20	Becker et al. (2005)
B1929+10	8.1	5.2×10^7	250 ± 10	117 ± 6	0.01	250 ± 10	Przybyl et al. (2005)
B1929+10	85	5.5×10^7	<100	100.0	<0.001	<100	Przybyl et al. (2005)
B1929+10	34	7.4×10^7	180 ± 15	1.8 ± 0.1(0.1)	0.3	180 ± 15	This work
B1929+10	83	8.4×10^7	<100	100.0	<0.001	<100	McGowan et al. (2005)

